Neurophysiological models of gaze control in Humanoid Robotics

Manfredi, Luigi; Maini, Eliseo Stefano; Laschi, Cecilia

Published in:
Humanoid Robots

DOI:
10.5772/6728

Publication date:
2009

10

Neurophysiological models of gaze control in Humanoid Robotics

Luigi Manfredi, Eliseo Stefano Maini & Cecilia Laschi
ARTS Lab (Advanced Robotics Technology and Systems Laboratory,
Scuola Superiore Sant'Anna
Italy
manfredi@ieee.org

1. Introduction

Thanks to the improvements in mechanical technology, it is currently possible to design robotic platforms that are increasingly similar to humans (Laschi et al., 2008; Kaneko, 2004; Kuffner et al., 2005). However, the increasing robot complexity (i.e. presence of many degrees of freedom, non linear actuation and complex geometries), requires more sophisticated control models and heavier computational burden. The development of humanoid robot is a very relevant issue in robotic research especially when one considers the challenges related to the actual implementation of a humanoid robot both in terms of mechanics and control system.
However these research efforts are justified considering that, an actual humanoid robot is regarded as a fundamental tool for neuroscience and, at the same time, neuroscience can be exploited as an alternative control solution for the design of humanoid robots (Kawato, 2000).
In this chapter, the neurophysiological models for gaze (i.e. the line of sight) shift control will be discussed and their implementation on a head robotic platform is presented. In particular the rapid movement of the gaze and the issues related to the eye-head coordination were investigated from neurophysiologic and robotics points of view. In neurophysiology the rapid movement of the gaze is known as *saccadic*. This movements are also classified either as *head-restrained* visual orienting movement or *head-free* visual orienting movement (Barnes, 1979; Bizzi et al., 1971; Bizzi, 1972; Guitton andVolle 1987; Guitton, 1992; Goossens and Van Opstal 1997).
The neurophysiologic models that will be discussed here are the visual mapping of superior colliculus and the independent gaze control model presented by Goossens and colleagues for the eye-head coordinated motion (Goossens & Van Opstal, 1997).
In the case of visual colliculus mapping, the input is a visual image that is mapped from camera image to the superior colliculus. Conversely, for the gaze model control, the input data are the two angular deviations (i.e. horizontal and vertical) that may be used to define the gaze shift amplitude and the movement orientation. The eye-head saccadic model

presented here derives from the one proposed by Goossens and Van Opstal with the aim of controlling both the eye and head movements.
The experimental setup was designed to test two typologies of results. One is the capability of reproducing the human behaviour both in terms of movement and velocity profile (i.e. velocity peak and movement duration for eye, head and gaze related to the displacement). Secondly, stability and response time have been measured in order to assess the ability of the model to control a redundant robotic platform.
The reported results show that, the visual target is properly achieved and its stability is maintained with low residual oscillation. Some limits have been noted in the beginning of the head movement when the amplitude of the movement is small. However, the obtained results are similar to humans (Goossens and Van Opstal, 1997). We are aware that higher repeatability and accuracy may be achieved by using the traditional control; however the residual errors of movements are lower or equal to those reported in neurophysiologic studies. Moreover, the impressive human like appearance of the motion obtained with this model can encourage its use in the design of more "social robot".
Future work could include the implementation of a dynamic model and the inclusion of an automatic learning phase of models gains.

2. Physiological models

The objective of studying physiological behaviour is to formulate a model description of the target - *black-box model* - (defined as $G(s)$, where s is the Laplace variable). This is a classic model identification problem.
Usually, a general physiological system is composed of many sub-models interacting with each other. Therefore, in order to be able to identify and exploit a particular sub-model, it needs to be isolated. The physiological models can be divided in two main categories: *qualitative*, and *quantitative.*
The *qualitative models*, often formulated by biologists, provide a description of the model behaviour by means of input-output relations.
Conversely, the *quantitative models* provide the mathematical formulations of the physiologic model. In this case, the system can be simulated and tested. Finally, real data can be compared with results in order to assess the ability of the model to describe the real system.
In recent years, the increasing computational power allows the simulation of more complex mathematical models, giving rise to more effective investigations. Accordingly, mechanical and electronic improvements have given the opportunity of building robotic platforms more similar to biological systems. Therefore, in these days we assist the birth of a new area research at the bridge of robotics and neuroscience. Its main goal is to use real robotic platforms to (1) validate the investigated model, and (2) use the proposed model to control a complex and redundant platform. The latter, can be used as an alternative way to the traditional control approach.
The classical control theory gives the possibility of being more accurate when the problem is mathematically identified. Indeed, the physiological approach is less accurate and repeatable. However, the particularity of physiological approach is the capability of generalizing and controlling a system with slow sensory response. Many physiological studies suggested that prediction is used in many tests for compensating slow sensory response (Wolpert and Kawato 1998).

There are two types of control based prediction:

- using motor commands to achieve a desired output;
- predicting the output obtained from the given motor command.

In the first case, the input of the prediction model is the desired task output, and it provides the motor commands required to accomplish the task. In this case, the prediction is made by identification of the inverse system model ($\hat{G}(s)^{-1}$).

In the second case, the input is the motor commands, and the prediction model provides the future output of the system.

In this case the prediction is made by identifying the model of the system: $\hat{G}(s)$.

Investigation of such problems is inherently complex hence a multidisciplinary group is fundamental; this should include biologists, physiologists, neuroscientists and engineers.

3. Ocular movements

In human as in primates, vision is based on images with a space-variant resolution. The photosensitive area of the eye is characterized by a non-uniform density of photo receptors (Green, 1970). The central part of the retina within 5 deg, is known as *fovea*, which has much higher resolution than the periphery. Thus, the target object needs to fall within the *fovea*. This implies the execution of many movements in eyes and head but in general also torso and limbs. The peripheral part has a resolution good enough to perceive visual stimuli, and the low quantity of information allows fast processing and especially fast visual-motor reaction. Both, the two eyes and the head compose the vision system. The *gaze* is defined as the eye position relative an external or spatial frame of reference.

How the brain transforms two-dimensional visual signals into multi-dimensional motor commands, and subsequently how it constrains the redundant degrees of freedom, are fundamental problems in sensory-motor control.

The common ocular movements are the following that are controlled by different part of the brain (Henn, 1993).

- *Microsaccades*: they are small, jerk-like, involuntary eye movements, similar to miniature versions of voluntary saccade.
- *Vestibulo-ocular reflex (VOR)*: is a reflex eye movement that stabilizes images on the retina during head movement, by producing an eye movement in the opposite direction of the head movement, thus preserving the image on the center of the visual field. It is a very reactive movement, with a latency (time between the head and the eye movement) of only 14 ms, guided by the vestibular system response, which detects head motion and posture. The VOR does not depend on the visual input and works even in total darkness or when the eyes are closed. It is considered as slow movement.
- *Optokinetic reflex (OKR)*: allows the eyes to follow objects in motion when the head remains stationary (and thus the VOR is not elicited) and it is activated when the image of the world slips on a large part of the retina; this reflex is based on the visual information and the latency is longer (100–150 ms) than in the VOR.
- *Saccadic movements*: are fast, ballistic, simultaneous movements of both eyes in the same direction. They can reach 800 – 1000 ◦/s, in a time of 30–120 ms (Bahill et al., 1975; Baloh et al., 1975);

- *Smooth pursuit*: is the ability of the eyes to smoothly follow a moving object. It is a slow movement.
- *Vergence movement*: is the simultaneous movement of both eyes in opposite directions to obtain or maintain single binocular vision. It is slower and can take up to 1s.

All movements of the eyes are in the same direction. Only the vergence makes an opposite movement of the eyes.
With regard to the neck, human motion is pretty complex, but three main movements can be identified (Zangemeister et al., 1981):

- Flexion/extension (i.e., ventral or dorsal flexion of the neck).
- Lateral bending (i.e., right and left flexion of the neck).
- Axial rotation (i.e., right and left rotation of the neck on the vertical axis).

Table 1 reports data on performance of human eye and neck movement, in terms of ranges of motion of cervical spine segments (ROM), maximum speed (VMax) and maximum acceleration (AMax) (Zatsiorsky, 1998).

Joint	ROM (deg)	*V*Max (deg/s)	*A*Max (deg/s2)
Neck lateral bending	−27/+27	100	1000
Neck flexion/extension	−45/+54	100	1000
Neck axial rotation	−58/+58	200	3000
Eye pitch	−40/+40	700	12000
Eye yaw	−45/+45	700	12000

Table 1. Human eye-head data performance: amplitude (ROM), maximum speed (VMax) and maximum accelerations (AMax).

Therefore, both the eyes and head can rotate about three mutually perpendicular axes: horizontal rotations about a vertical axis, vertical rotations about a horizontal axis, and torsional rotations about a naso-occipital axis.

4. Gaze movements

The saccadic and head-eye saccadic movement can be driven by different stimuli: visual, auditory, tactile or olfactory. The stimulus coordinates need to be converted in the retina reference system. In the case of visual stimulus, the retinal error drives the movements.
The main problem is how the saccadic system maps from two-dimensional (2-D) of retinal target error in to 3-D rotation of the eye and head. Indeed, the eye has 3 degree of freedom (DOFs) and another 3 DOFs for the head (excluding head translational movements). Therefore, the mapping is from 2-D to 9-D and it must preserve eyes and head mechanical constrains. The most important constrain is that the *eye-in-head* must obey Listing law (Radau et al., 1994) and the *head-on-torso* must obey Donders law (Radau et al., 1994). However there is a problem of redundancy that the brain solves in slightly different ways for the eyes and the head (Bernstein, 1967; Crawford et al., 2003).

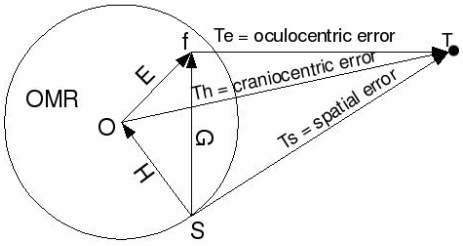

Fig. 1. Reference frame coordinates. T is the target stimulus, S, O, f are respectively the external reference frame (inside oculomotor range OMR), head end eye reference system. G represent *eye-in-space*, H *head-in-space*, E *eye-in-head*. **Te** is the *target-in-eye*, **Th** *target-in-head* and **Ts** *target-in-space*.

If the target is indicated with **T**, the craniocentric error is **Th,** spatial error **Ts** and oculocentric error **Te.** The eye displacement is **Te=Th-E**.
Two main approaches are followed to investigate the gaze control model:

1. head-restrained visual orienting movements: *eye saccadic movements*;
2. head-free visual orienting movements: *eye- head saccadic movements*;

Actually, the movement is more complex because also the torso and limbs interact with the movement.
This kind of control is obtained by transforming position into motor activation (in time) which is a function of time. This is the so called *spatio-temporal transformation* (STT) (Sparks, 2002).

4.1. Head-restrained visual orienting movements: *saccadic movements*.

When the head is fixed, the gaze is performed by rapid eye movements that can be accurately predicted, if the amplitude and direction are known, in term of duration and peak velocity (Bahill et al., 1975; Baloh, 1975). The relationship between duration and saccadic magnitude is linear (VanGisberg and Johnson, 1984). The latency saccadic period depends on the stimulus (source and intensity Bell et al. 2006).
Moreover, when this criterion is not respected, often a neuromechanical deficit is present (Westheimer and Brail, 1973; Zee et al., 1976).

$$V = \alpha(1 - e^{-\frac{x}{\beta}}) \tag{1}$$

Equation (1) shows the relation between eye velocity and eye amplitude where V is the maximum velocity, x the saccadic amplitude α and β are the parameters of the exponential model which can be calculate as the minimum of the square error between the model and the data (Baloh et al., 1975; Collewijn et al., 1988).
An example of saccadic movement is shows in Fig. 2

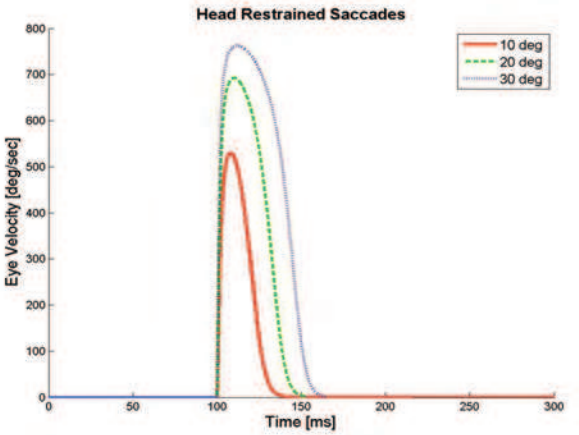

Fig. 2. Velocity profile of saccadic movement. The delay of activation strictly depends on stimulus source and intensity.

Many saccadic models have been proposed with the aim of understanding how a more simple system acts, e.g. an eye, in order to understand how a more complex system (e.g. a limb, which use multiple joints and operate with varying loads) is controlled.
The saccadic system is under a continuous feedback control. The main question is what the source of the feedback is. Cannot be visual because the retina signal is too slow compared to the saccadic dynamics. Many hypothesis and many models have been formulated (Robinson, 1975).
Many parts of the brain are involved in transforming the visuo-information provided by the retina in to the motor-neuron activation (STT). The main problem is to understand which the control strategy is; whether it is feed-back or feed-forward based, considering that the movement is very fast and the signal transmission is slow.
One of the first models formulated by Robinson (Robinson, 1975) supposes that the saccadic movements work as non ballistic systems actuated by a feed-back loop. The feed-back is based on an efferent copy of the output of the saccadic burst generator, which is able to performance of on-flying correction of the trajectory.
Van Gisbergen and colleagues (Gisbergen et al., 1985) studied the dynamic of oblique saccades. They proposed that, in order to obtain a straight trajectory, the times needed to complete the two components of the movements are identical.
Tweed and Vilis (Tweed and Vills, 1985) extended the previous model by introducing of different gain constants for horizontal and vertical saccades, due to the probably different 3rd order dynamics of the eye muscles. In this model, it may be possible to have different dynamic calibration.
Grossberg and Kuperstein (Grossberg and Kuperstein, 1986), expanded the models of Robinson and colleagues by introducing a neural network model to actuate the antagonist eye muscles in the horizontal plane, instead of classic control approach.

4.2. Head-free visual orienting movements: *head-saccadic movements*.

When the gaze shift becomes large, the eye and the head work together. The oculomotor systems transformation the object position into target reference system and then in head reference system (Goossens and Van Opstal, 1997; Freedman and Sparks, 2000).
Many models of these transformations were formulated.
Bizzi and colleagues (Bizzi et al. 1971, Bizzi et al. 1972) proposed the so-called *oculocentric hypothesis*. According to this model, the head-free gaze is like the head-fixed gaze, independently of the occurrence and size of the concomitant head movement. The vestibulo-ocular reflex (VOR) is switched-off, and cancels any contribution of the head to the gaze. Several experiments showed that the VOR is more or less switched-off during saccades (Laurutis and Robinson, 1986; Pelisson et al., 1988; Lefevre et al. 1992). Further experiments validated this hypothesis for gaze shifts smaller than 10 degrees.
Differently from the head-fixed, in which the hypothesis of eye movements with local feedback of current position is accepted (Robinson, 1975), in the head-free model, it is supposed that the gaze motor-error drive the oculomotor system. According to this so called *gaze feed-back hypothesis*, the gaze saccades can be maintained even if the VOR is suppressed during the movement.
The main question is *what is the source of the feedback?*
As described in Fig. 3 two hypotheses are being explored. In the first hypothesis the gaze error, after decomposition in eye-error and head-error drives both, eye and head (Fig. 3-A) (Goossens and Van Opstal, 1997) . Differently in the second architecture, there exists only a local feedback of the eye-position whereas the head act in open loop (Fig. 3-B) (Freedman and Sparks, 2000; Freedman and Sparks, 1997).

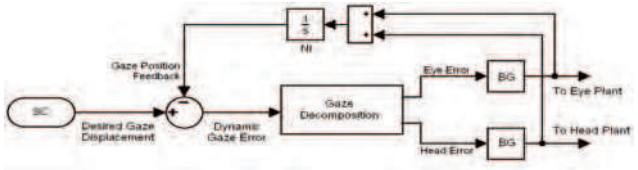

A)

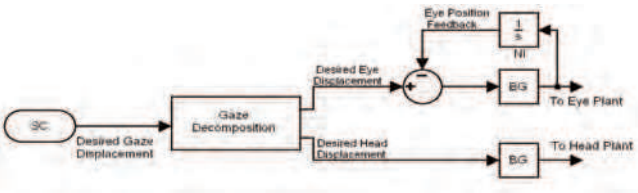

B)

Fig. 3. Two main hypothesis of gaze control architecture. **A.** The gaze error, after decomposition, drives both eye and head (Goossens and Van Opstal, 1997). **B.** After gaze displacement decomposition, a local feedback is present only in the eye. To identify the action of the feedback, several tests with external disturbance have been made (Freedman and Sparks, 2000). In both architecture (A-B) the system is robust to external disturbance.

Note that, in **B** architecture, the external disturbance is compensated making use of head and neck reflexes.

4.3.The collicular mapping of the visual field

Many models of collicular mapping have been proposed (see review of Girard and Berthoz 2005).

A critical structure in the gaze control circuitry is the superior colliculus of the midbrain. Indeed its deeper layers contain a retinotopically organized motor map in which each site is thought to encode a specific gaze saccade vector.

The way in which the mapping of the visual field occurs onto the SC was experimentally measured in primates by Robinson (Robinson, 1972) and subsequently mathematically modeled by Ottes and colleagues (Ottes et al., 1986). The equations introduced in (Ottes et al., 1986) for mapping the retinotopic coordinates (R,θ) onto the Cartesian plane (X,Y) of *the colliculus are*:

$$\begin{cases} X = B_x \ln\left(\sqrt{\dfrac{R^2 + 2AR\cos(\theta) + A^2}{A}}\right) \\ Y = B_y \arctan\left(\dfrac{R\sin(\theta)}{R\cos(\theta) + A}\right) \end{cases} \quad (2)$$

Where a = 3 deg, B_X 1.4 mm and B_Y = 1.8 mm. The expression of this mapping is rather complicated but it may be reformulated using complex logarithm in the following form:

$$\begin{cases} \dfrac{X}{B_x} + i\dfrac{Y}{B_Y} = \ln\left(\dfrac{z + A}{A}\right) \\ z = \alpha + i\beta \end{cases} \quad (3)$$

where α and β represent respectively the azimuth and the elevation of the saccade

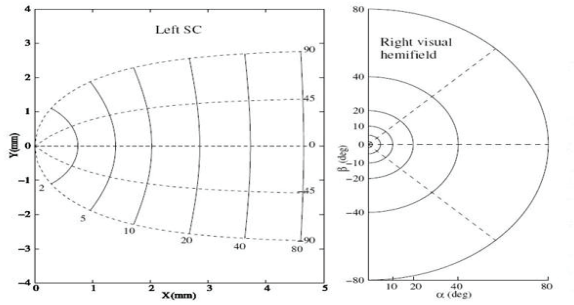

Fig. 4 The visual mapping from retina to colliculus.

The two right half sides of the retinas of the two eyes are projected onto the right SC, in the right side of the brain, while the two left half sides of the retinas of the two eyes are projected on the left SC.
Equation (3) has been use for collicular mapping software implementation.

5. Robotics application of gaze control

Eyes provide the ability to perceive and interact in unconstrained dynamics environments. This capability has been investigated in robotics as active vision. Several new researches have born to deep investigate this capability.
Many robotics applications have the scope to implement only fast eye movements useful for industrial applications and commercial vision systems. In this case relevant are the mechanical performance and the very fast control loop able to perform very fast movements.
From the viewpoint of social interaction, the robot has to give more social acceptability (Shibata, 2004).
Takanishi Lab of Waseda University, have developed a humanoid robot - WE-3RII - to mimic facial expressions, and saccadic movements have been implemented, with the same delay of human ones, with the purpose to facilitate social interaction (Takanishi et al., 1999).
Instead, studying the modeling and validation of neurophysiological models gives two possibilities: to understand how the models are correctly implemented and how it can be possible to control a robotic platform.
Clark and colleagues (Clark, 1998) have implemented, in a simple pan-tilt camera, a spatial attention mechanism with related saccadic camera motion. They have implemented a non programmed saccadic movement based on the pattern activity of the attention mechanism, based on winner-take-all model.
Ferrell (Ferrell, 1996) has implemented a saccadic system based on Self Organizing Maps (SOM) on the Cog platform (Brooks et al., 1999). By using feedback error-learning (model formulated by Kawato (Kawato et al., 1987))
Bruske and colleagues (Bruske et al., 1997) have proposed an adaptive saccade model for a 4 DOFs binocular camera head. The goal was not to emphasize the biological model, but to improve a real-time architecture based on a small neural network.
Panarei and colleagues have implemented image stabilization by using a bioinspired solution. It was implemented by using two sensors, inertial and visual (like vestibular and optokinetic in nature). The relations between sensors and system control are obtained by the process of learning of a neural network.
Berthouze and Kunihoshi (Berthouze & Kuniyoshi, 1998) have demonstrated the learning by neural network of sensory-motor coordination (i.e. VOR and OKR) by a 4 DOFs robot head.
Manfredi and colleagues (Manfredi et al., 2006) have implemented an eye-saccadic model in an anthropomorphic robotic head. The model has been implemented in the robot in order to validate it.
Preliminary experiments on eye-head coordination models were already performed by Maini and colleagues (Maini et al., 2008) on a anthropomorphic robotic head.
Many works have not remarked the robotic implementation, which contribute for investigating the validity of the implemented model. The main issue is how the robotic

platform can be used to validate the neurophysiological model. Often, a simulation is not complete enough to investigate the real behaviour of the studied model.
In many cases, the robotic platform is non adequate because it has less DOFs or less performance respect to the real biological platform.
In the present work two main points are emphasized: (1) the performances of the robotic head (Laschi et al. 2008) in terms of dynamics are quite similar to human data available from literature (Zatsiorsky, 1998); in this way it is possible to duplicate the neurophysiological models; (2) investigating the validity of the proposed model (according to 2-D independent gaze control hypothesis formulated by Goossen and Van Opstal (Goossens & Van Opstal, 1997)) to control a redundant robotic platform and to obtain results comparable to literature data.

6.Experimental Validation

6.1.Overall system

Fig. 5 represents the overall system architecture. The fast gaze shifts were evoked by presenting a visual stimuli to the robot that executed the task according to the following step: selection and detection of the color of interest; mapping of the image onto the collicular; estimation of the stimulus center of mass. The elevation and the azimuth of the stimulus were then passed to the eye-head coordination model that generated a velocity profile with a sampling time of 3 ms.

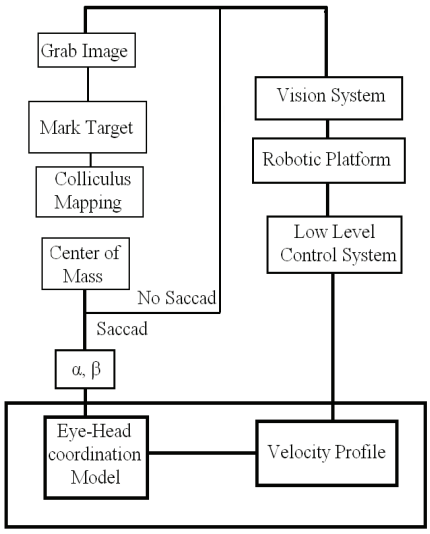

Fig. 5. Overall system architecture. After traditional color edge detection, the selected target is mapped in the superior colliculus. Then, the centre of mass of the mapped stimulus is detected and, it is send to the eye-head model which provides the velocity profile. The communication protocol is the TCP/IP. On the robotic head platform, the server application receives the data with a sample time of 3 ms.

6.2.The robotic platform and the vision system.

The robotic platform used for validating the system has been composed of 7 DOFs (Fig. 6). It is composed of two parts: a neck and a head. The neck has 4 DOFs respectfully 2 in the lower part (roll and lower-pitch) and last two in the upper part (upper pitch and yaw). The head has 3 DOFs, 1 common for the two eyes (pitch) and the last, one for each eye (yaw left and right). All the system has been controlled by an embedded PC where a server application has been implemented. The main characteristics of this hardware are the capability to perform the dynamics quite similar of human head. The robotic head performances are show in Table 2.

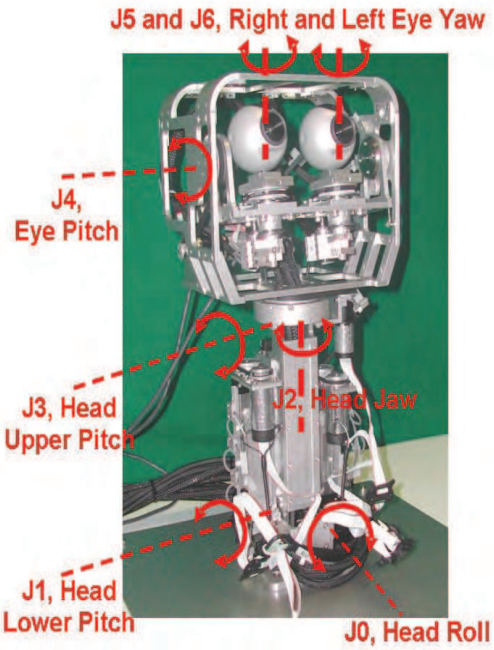

Fig. 6. Robotic platform composed of 7 DOFs. The neck has 4DOFs, two in the lower part (roll and lower-pitch) and two on the upper part (upper-pitch and yaw). The eyes have 3 DOFs, one common pitch and 1 yaw for each eye.

JOINT	ROM [deg]	V_{MAX} [deg/s]	A_{MAX} [deg/s^2]
Roll	± 30	25	200
Lower pitch	± 25	20	200
Yaw	± 100	170	750
Upper pitch	± 30	120	750
Eye pitch	± 47	600	4,500
Right Eye Yaw	± 45	1,000	10,000
Left Eye Yaw	± 45	1,000	10,000

Table 2. Robotic head ranges of motion (ROM), maximum speed (VMAX) and acceleration (AMAX).

Each eye has one commercial USB webcam, with the resolution of 640x480 pixel and 30 frame per second.
The robot is controlled using a PID (proportional, integrative and derivative) implemented in a DSP (Digital Signal Processor) motion controller (MEI 104/DSP-400 by Motion Engineering Inc, USA). Two boards are present, one for 4 axes and another for 3 axes. A software limit switch prevents mechanical injury. The axis control board is connected by PC104 bus in a Pentium IV PC, 3.0 GHz.
A *server application*, implemented in C++, receives and sends the command to control the robotic platform by using TCP/IP protocol. Therefore, the model implemented as *client application*, can run in the same PC or on other.
For more detail refer (Laschi et al., 2008).

6.3. Implementation of the Superior Colliculus mapping

It is worth noticing that, a straight use of this transformation for obtaining the collicular mapping may introduce some relevant ambiguities in real-world applications. Indeed, the CCD cameras have a uniform discrete pixel distribution whereas the equation (3) and (2) are defined on a continuous domain. Therefore, it is obvious that the logarithmic function will map the discrete points of the retinotopic plane in such a way that will spread the pixels pertaining to the central part of the collicular map. Conversely, in the peripheral part of the collicular map the density of pixels will be increased with a subsequent loss of information. To avoid this problem a void collicular map has been started from and for each pixel in the collicular map has been back-projected the coordinates onto the retinotopic plane making use of the equation (3) as reported in (Girard & Berthoz, 2005). Obviously, the results (as X_c, Y_c, coordinate in camera reference system) will be, in general, not integer hence with no physical representation on the CCD matrix. To solve this ambiguity we associated to the virtual point X_c, Y_c an intensity value that was calculated using a weighted interpolation of the surrounding four connected integer pixels. Finally, it has imposed the latter intensity value to the original point of the collicular map and we iterated this procedure for each point on the collicular plane. An example of the resulting well smoothed collicular maps is reported in Fig. 7.

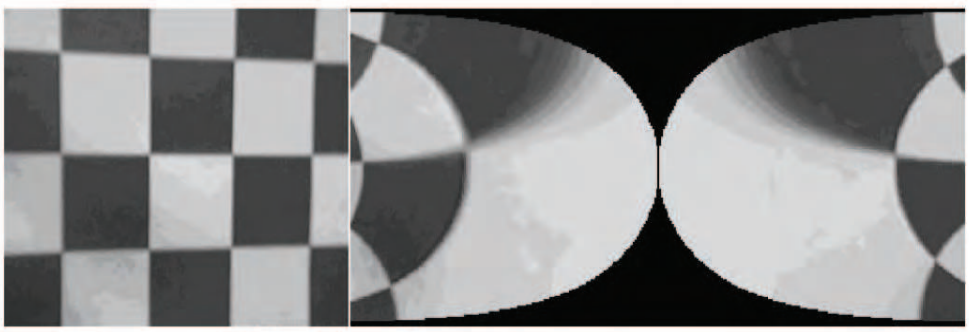

Fig. 7. Collicular mapping according to equation (3) with interpolated uniform resolution. **Left**: the image acquired by the camera; **Right**: the two halves of the image mapped with the collicular geometry expressed by equation. (3).

6.4. Stimulus detection

Visual stimuli are detected in the collicular image, as obtained after collicular mapping, by means of a color-based threshold algorithm. Specifically, the detection of the stimuli is performed with a simple procedure of color recognition based on a target color manually indicated.

The procedure makes use of the HSV (hue, saturation and value) color representation, instead of the classical RGB (red, green, blue), in order to improve the robustness with respect to light variations. After the detection of the selected color, the centroid of the object is calculated and the coordinates on the collicular plane are fed to the model, in order to produce the velocity profiles for controlling the motion of the eyes, similarly to what happens in humans.

In Fig. 8 is a show an example of stimulus detected after mapping and before gaze performed and in

Fig. 9 after gaze performed.

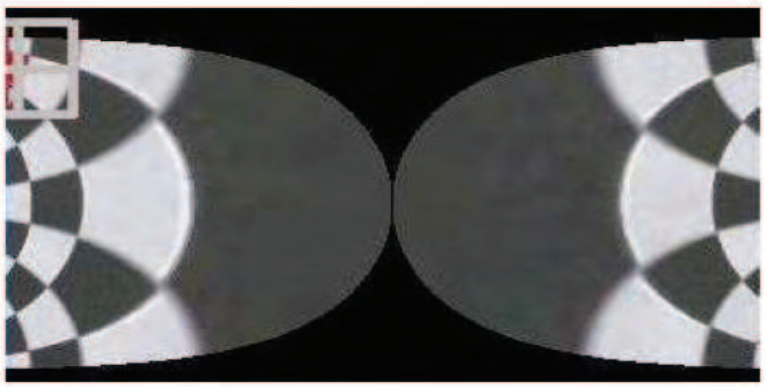

Fig. 8. Collicular mapping of the detected stimulus: the centroid of the object is marked with a targeting square on the collicular plane.

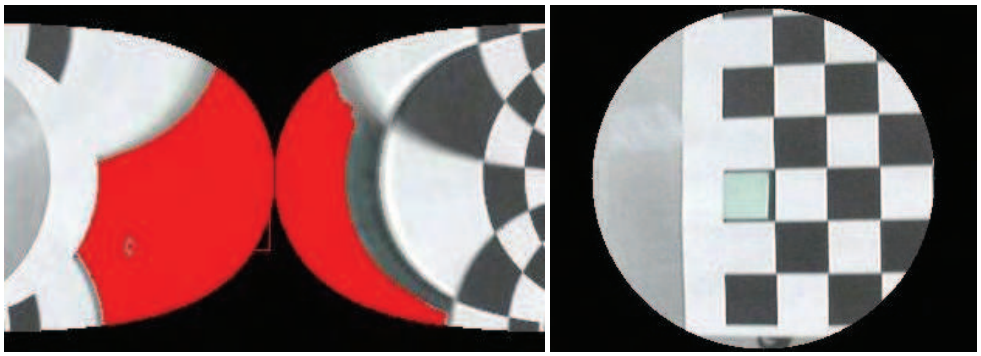

Fig. 9. The collicular mapping of the foveated object (left) and the visual field of the robot after the saccadic movement (right).

6.5. Model implementation

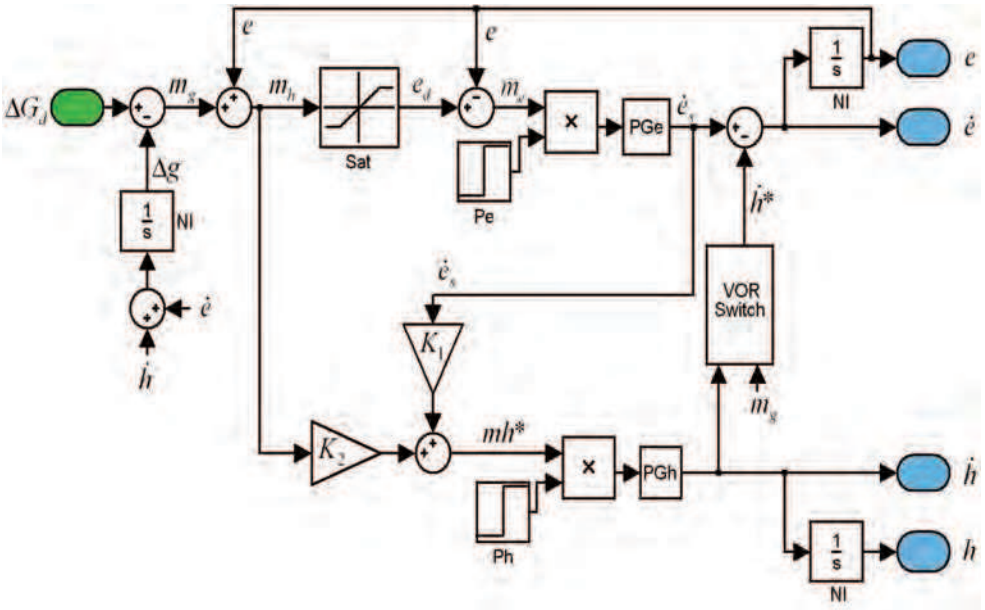

Fig. 10. The independent 2-D gaze control model as proposed in Goossens and Van Opstal (Goossens and Van Opstal, 1997), implemented in Matlab Simulink real-time. It is based on current gaze displacement feedback (modified after Guitton and Volle 1987 (Guitton & Volle, 1987)). ΔG_d is the target amplitude provided by superior colliculus (SC). Semicircular canals (SCC) provide the head velocity $\dot{H}$. The PG_h and PG_e blocks represents the head and eye pulse generator. **Sat** block, identifies the eye constraint. K_1 and K_2 define the head displacement decomposition. **VOR-Switch** represents the VOR behaviour.

A desired gaze displacement ΔG_d is given as input to the model and compared to current gaze displacement Δg (*eye-in-head* + *head-in-space*). The gaze displacement is obtained as integration (*rst* reset the integration of $\dot{g}$ after each saccadic movement) of eye ($\dot{e}$) and head ($\dot{H}$) velocity (provided by semicircular canals SCC - **VOR-Switch**). The residual displacement, is converted in head-motor error m_h. Initially **me** and **mh** are identical to the oculocentric and craniocentric target coordinates (**Te** and **Th**, see Fig. 1). The **Sat** block is to limit the eye mechanical constrain. Then, the desiderate eye position (e) is compared to current eye position and driving the eye as local feedback (as Robinson's local feedback model Robinson1975). Than, it is compared to current eye position. The head velocity,

provide from SCC, after a partial attenuation ($\dot{h}^*$), interacts downstream from the eye pulse generator. In our implementation, because robotic platform fixed, the SCC is the actual velocity provided by axis control board. The eye and head movements can be controlled by separate gating mechanisms as possibility to test difference delay likes visual and auditory source.

The **VOR-Switch** block, has been implemented for deep investigate of its role. Until now, it is not clear how the VOR is implicated in the head-saccadic movement. It is know, from literature data, that it is weakened or shut off in the direction of the saccade. But it is not clear if it is shut-off in the direction of the *gaze* (*eye-in-space*) or *head-in-space* or *eye-in-head* motor error.

The model implemented is based as different timing:

1. **t=0** : the ΔG_d value is send to the system:

The input signal ΔG_d drives the system. The onset of the eye and head movement depends as source (Bell et al., 2006). The time can be defined by setting **Pe** and **Ph** delay variables.

2. **t=Te+** : the eye starts to move:
3.

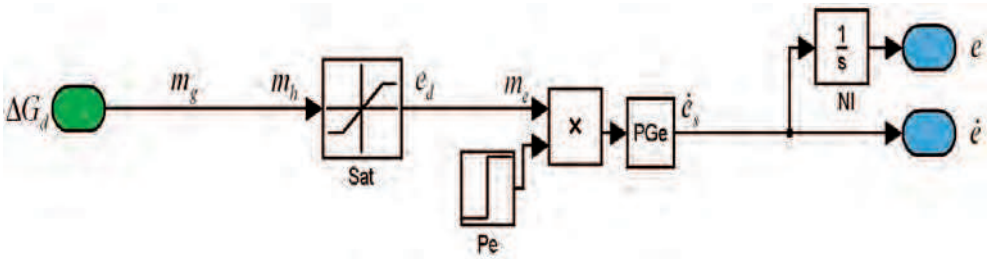

Fig. 11 Block diagram of the model at the time **t=Te+**

The eye movement starts onset of **Pe** block. The system is shown in Fig. 11.The eye has not received any feedback and it starts to move as open-loop system. The **PGe** block (eye pulse generator) is activated and provides the eye velocity. This is sent to the robotic platform, and it starts to move according to mechanical dynamics. The eye constrains is defined in **Sat** block.

4. **t>Te** : the feedback eye starts:

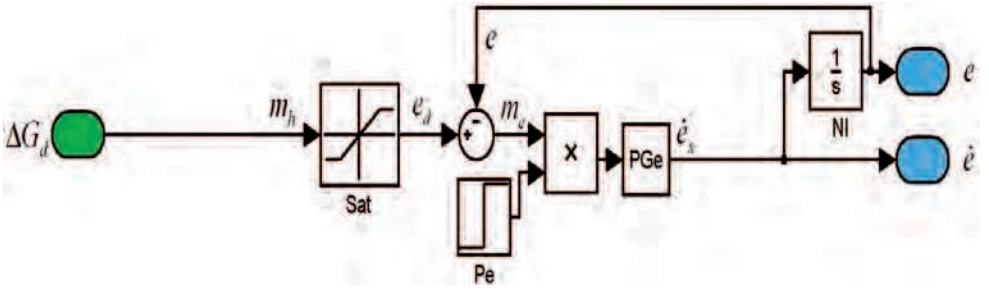

Fig. 12. Block diagram of the model at the time **t>Te**

In this phase (see Fig. 12), the eye starts to move as eye-saccadic movements according to Robinsons' local feedback model (Robinson, 1975). The ΔG_d , after saturation block (**Sat**, according to mechanical constraint), is sent to the **PGe** block which provides the velocity command to the eye. The eye perform the gaze shifting as own system, without head. In this condition, the eye starts to move according to maximum velocity performance. **PGe** block has been implemented concerning traditional used model (Becker & Reinhart , 1990) shown in equation (4). The equations (4) show the system equation.

$$\begin{cases} \dot{e} = PG_e(m_e) = K \cdot (1 - e^{-(\frac{m_e}{10})}) \\ me = e_d - e \\ ed = Sat(m_h) \end{cases} \quad (4)$$

5. **t=Th+** : the head starts to move:

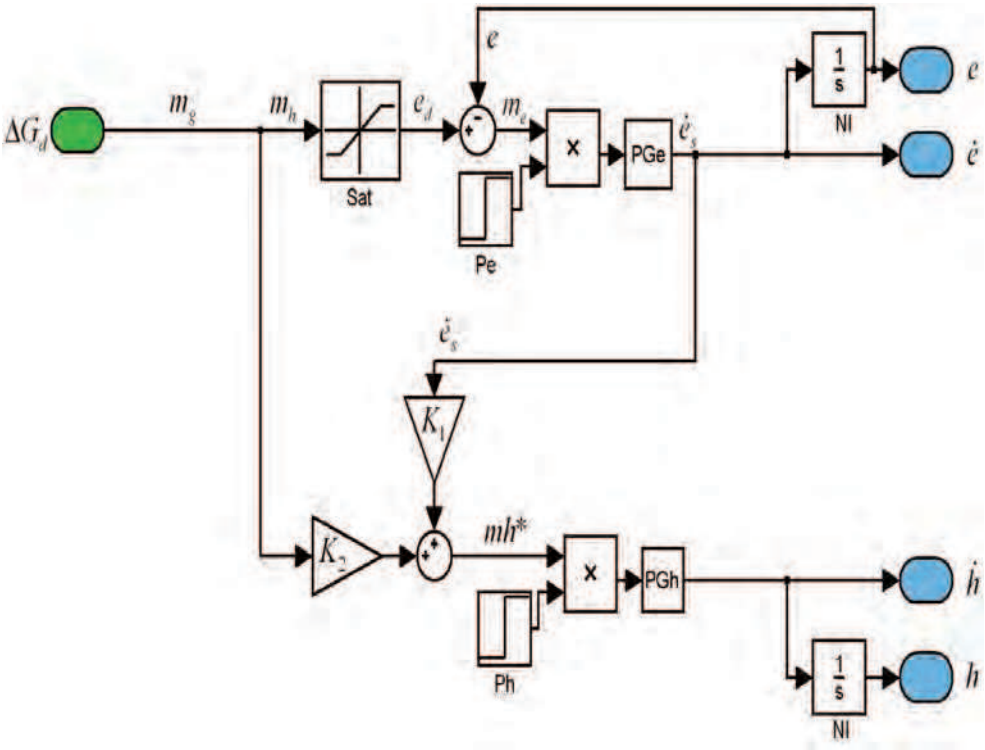

Fig. 13. Block diagram of the model at the time **t=Th+**

The mh^* is sent to the PG_h block (head pulse generator) and the velocity command $\dot{h}$ is sent to the robotic platform. The head starts to move according to mechanical dynamics. As shown in equation (5), the head has to perform the residual displacement error, until not performed by the eye. The block diagram is shown in Fig. 13.

$$\begin{cases} \dot{h} = PG_h(mh^*) \\ mh^* = K_1 \cdot \dot{e}_S + K_2 \cdot \Delta G_d \end{cases} \quad (5)$$

6. **t>Th** : the feedback head starts:

At this stage, the head is already started and the system is going on. The block diagram is shown in Fig. 12.

$$\begin{cases} \dot{h} = PG_h(mh^*) \\ mh^* = K_1 \cdot \dot{e}_S + K_2 \cdot m_h \\ m_h = e + m_g = \Delta G_d - h \\ m_g = \Delta G_d - \Delta g = \Delta G_d - (e + h) \\ \Delta g = e + H \end{cases} \quad (6)$$

In conclusion, the results of the model are strictly dependent on the given gain. Also the low level control (i.e. capability to fix the velocity profile provided by the model) influences the behaviour.

7.Experimental trial

The experiments and the setting of the system gain have been done to imitate the data reported in the Goossens and Van Opstal work (Goossens and Van Opstal, 1997).
The experiments were performed by positioning a visual stimulus (i.e. a green ball) in the robot's field of view and by recording (from the encoders) the actual positions of the involved joints. In the starting position, the eyes and the head were aligned. The position of the stimulus was then varied in order to span the entire visual field of the robot. In order to test the effectiveness of the model on a wide spectrum of movements the amplitude of the gaze shifts required to foveate the target was varied from 5 deg up to 35 deg for horizontal saccades. Several different trials were performed for each tested amplitude.
The model has been tested (1) to investigate the robot performance and compare them to physiological results and, (2) to test the capability of the model to control a redundant robotic platform using a neurophysiological model. Fig. 10 shows a typical example of head-saccadic movement.

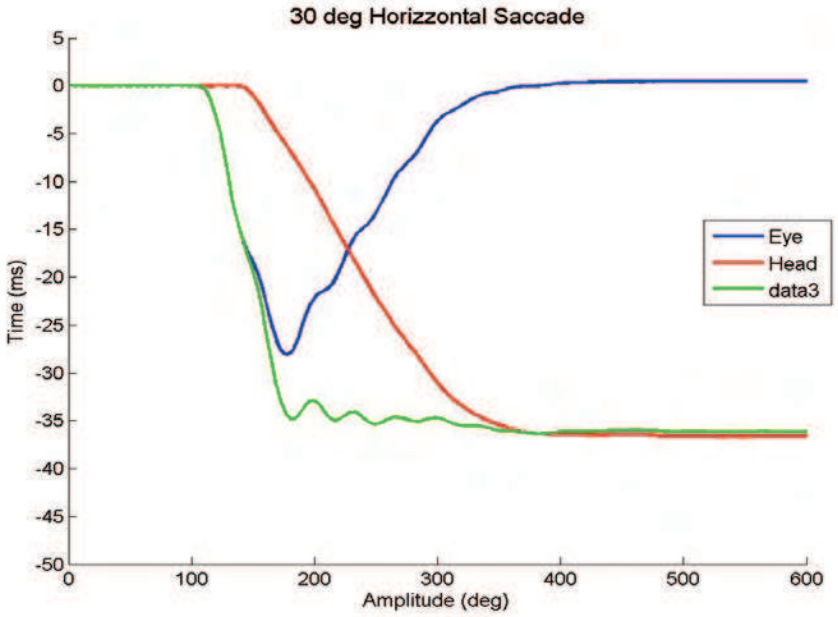

Fig. 14. Example of robotic head execution of 30 deg head-saccadic movement.

In the reported data, the zero time point is calculate from the onset of the **Pe** delay block.
To test the system performance, the following outcome measures were calculated:

Timing measures:

Gaze:

- **TGS10**: time to achieve 10% of final **gaze** displacement;
- *duration* **TGD**: time to achieve 90% of final **gaze** displacement;
- *delay time* **TGri**: time to achieve 50% of final displacement;
- *settling time* **TGst**: time to reduce the gaze oscillation below the 5% of the final displacement;
- **Tg** *gaze duration*: time between the gaze movement onset, **TGS10**, and the target achievement **TGS90**.

Head:

- **THS10**: time to achieve 10% of final **head** displacement;
- *duration* **THD**: time to achieve 90% of final **head** displacement;
- *delay time* **THri**: time to achieve 50% of final displacement;
- *settling time* **THst**: time to reduce the head oscillation below the 5% of the final displacement**;**
- **Th** *head duration*: time between the gaze movement onset, **THS10**, and the target achievement **THS90**.

Eye:

- **TED**: time to change the eye velocity sign (eye duration).

Velocity peak measures:

- **PVG**: gaze peak velocity;
- **PVH**: head peak velocity;
- **PVE**: eye peak velocity.

8.Results

The obtained results are shown for horizontals movements in table 4.

Fig. 15 shows the main sequence relation for the gaze, eye and head movements.
The main results are shown in Figure 16, 17.
Reported data are intended to investigate to different behaviors:

(1) accordance with the data provided from Goossens and Van Opstal study (Goossens and Van Opstal, 1997);

(2) capability to control the redundant robotic platform.

The first point is discussed in reference to the available data of eye and head coordination as reported by Goossens and Van Opstal study (Goossens and Van Opstal, 1997).
The second point has been tested, using traditional methods: timing response, residual oscillation for eye, head and gaze.

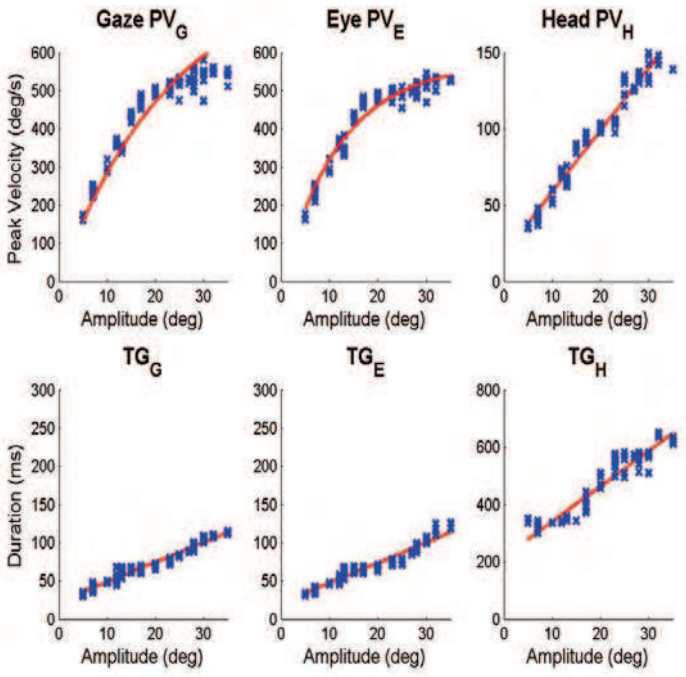

Fig. 15. Saccadic kinematics. Duration and peak velocity as a function of amplitude for gaze, eye and head. **PVG**, **PVE**, **PVH** are the peak velocity of the gaze, eye and head. **TGG**, **TGE**,

TGH are the movements duration of the gaze, eye and head. Goossens and Van Opstal obtained close results (Goossens and Van Opstal, 1997).

	Duration	**Peck Velocity**
Gaze:	$TG_G = 22.92 + 2.56 \cdot A$	$PV_G = 610 \cdot (1 - e^{-(\frac{A}{13.32})})$
Eye:	$TG_E = 20.06 + 2.67 \cdot A$	$PV_E = 573 \cdot (1 - e^{-(\frac{A}{12.25})})$
Head:	$TG_H = 216 + 12.34 \cdot A$	$PV_H = 18.04 + 4.05 \cdot A$

Table 3. Fitting equations of linear and exponential model for peak velocity and duration related to displacement. The eye and gaze data are fitted with exponential equation because the maximal velocity has been achieved.

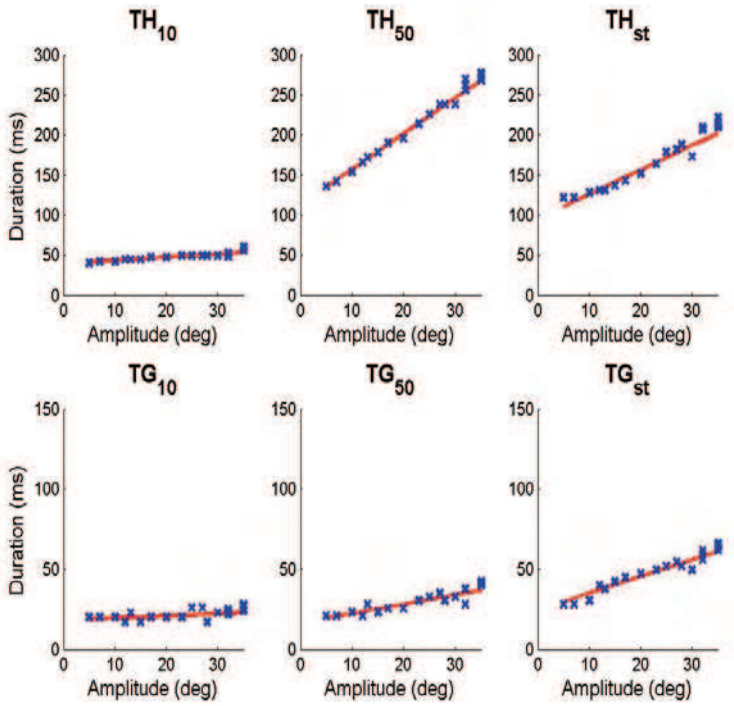

Fig. 16. Saccadic timing. Duration of **TH10**, **TH50**, **THST**, **TG10**, **TG50** and **TGST** as a function of amplitude for head and gaze.

	T10	T50	TST
Gaze:	$TG_{10} = 18.1 + 0.13 \cdot A$	$TG_{50} = 16.6 + 0.58 \cdot A$	$TG_{ST} = 24.2 + 1.05 \cdot A$
Head:	$TH_{10} = 39.5 + 0.4 \cdot A$	$TH_{50} = 111 + 4.46 \cdot A$	$TH_{ST} = 95 + 3.04 \cdot A$

Table 4. Fitting equations of linear and exponential model for peak velocity and duration related in related to displacement.

9. Discussion

This work present a robotic implementation of a neurophysiological model of rapid orienting gaze shifts in humans, with the final goal of model parameters validation and tuning. The quantitative assessment of robot performance confirmed a good ability to foveate the target with low residual errors around the desired target position. Furthermore, the ability to maintain the desired position was good and the gaze fixation after the saccadic movement was executed with only few oscillations of the head and eye. This is because the model required a very high dynamic.

9.1. Robotic point of view

The head and eye residual oscillations increase linearly with increasing amplitude. In Fig. 16 is evident that the residual gaze oscillation is less than head. This is explained with the compensation introduced by the eye oscillations which compensate the gaze which becomes more stable.

We explain these findings by observing that the accelerations required to execute (or stop-and-invert) the movement are very high especially for the eye movement. Even if the robotic head was designed to match the human performances (in terms of angle and velocities) in its present configuration it is still not capable produce such accelerations. This is particularly evident for the movement of the eye because the motor has to invert its rotation when the fixation point is first achieved.

With respect to the timing of the movement it has been found that the results of the experiments are in close accordance to the data available on humans (Goossens and Van Opstal, 1997). The same conclusion may be drawn for the shapes of the coordinated movement that can be directly compared to the typical examples reported in Fig. 14.

Figure 16, 17 show that the model is capable of providing inadequate control of the redundant platform.

The system response is very fast, due to the robotic head platform design.

TGst time take into account the problem of eye-head coordination and the very high acceleration.

The head is voluntarily delayed less than 30 millisecond after eye movement, according to human physiology, by means of **Ph** block (Goossens and Van Opstal ,1997).

9.2. Neurophysiological point of view

A typical robotic eye-head movement is shows in Fig. 14.

Very similar kinematic profile can be observed in neurophysiological studies on human (CITE CON PROFILI). The model drives the gaze by means of the global error displacement. Therefore, if an external disturbance has been applied, the oculomotor system reacts by compensating the gaze error.
The VOR plays an important role for the architecture behaviour. Therefore, a VOR block has been created to build different behaviour inside.
The obtained timing is in good accordance with human physiology reported in Goossens**.**
In the presented model, different eye dynamics may be obtained by modification of **PGe** block.
If the head is disabled by shutting off the **PGh** block, can be also possible to implement an eye-saccadic movement within the head-restrain paradigm.
In this case the model is in good accordance with Robinsons' local feedback model (Robinson, 1975)
Concerning the relation within peak velocity and gaze amplitude, it may be noted the close similarity between gaze and eye. This is explained with the preponderant role of the eye.
Conversely, the head velocity is linear because of the slow response as compared with the eye peak velocity.
As for the gaze duration, eye, head and gaze show a linear relation with gaze amplitude.
The different duration are explaining with the different dynamic.
The equation (7) shows the relation between peak velocity and displacement both for the gaze and eye. This is in exponential form in which V_p is the peak velocity, A the movement amplitude, and the constant to be fitted are V_M (the maximal eye velocity) and A_0 (that define how the system become saturated).

$$V_p = V_M \cdot (1 - e^{-(\frac{A}{A_0})}) \tag{7}$$

In the first part, below 400 deg/sec, the relation is almost linear, but, for increasing velocity it tends to be saturated for the achieved of limit velocity. The gaze is quite similar to the eye because, in this range, the eye plays the main role in the movements. Conversely for the head, the peak velocity is linear, because the different inertial properties of the head.

10. Conclusion

In our vision these results encourage the accomplishment of focused experimental trials in which the robot behaviour can help investigate the accuracy of the model (e.g. by varying the loop-gains) - and to possibly revise it - with respect to human behaviour in head-saccade execution.

This work may be considered the first preliminary attempt to reproduce the neurophysiologic model of human gaze control on an actual robotic artifact. However the obtained results are in close agreement with reported results on human's experiments both in terms of peak velocity and gaze duration (Goossens and Van Opstal, 1997). Moreover,

from a robotics point of view, this model has proved to perform an adequate control of a redundant robotic platform.

Nevertheless we are aware that future research activities should be devoted to the possible improvement and amelioration of the proposed model. Specifically, we envisage two strategic lines of research. On one hand, supplementary research activities should be dedicated to a better understanding on how the VOR interacts with the saccadic movement. Indeed, as already remarked, the VOR is known to be weakened or shut off in the direction of the saccade, but it is not clear if it is shut-off in the direction of the gaze (eye-in-space) or head-in-space or eye-in-head motor error.

On the other hand, we remark that the acquisition of coordinated motion of the eye and the head is a developmental issue. For instance, in newborns gaze shifts towards auditory of visual stimuli are absent or improperly accomplished until the development of appropriate strategies which occurs at about 6-9 months of age. This observation leads to the conclusion that –in humans- the model internal parameters should be learned by execution. Accordingly, a possible improvement of the model may include the introduction of adequate artificial neural network for learning the internal model parameters. This may be accomplished –for instance- by minimizing the error existing between actual and target kinematics until convergence of the network.

11. References

Bahill, A.; Clark, M. & Stark, L. (1975). The main sequence, a tool for studying human eye movements, *Math Biosciences*, Vol. 24, (1975), pp. 191-204.

Baloh, R. (1975). Quantitative measurement of saccade amplitude, duration, and velocity, *Neurology*, Vol. 25, No. 11, (1975), pp. 1065-1070.

Baloh, R.; Konrad, H.; Sills, A. & Honrubia, V. (1975). The saccade velocity test, *Journal Neurology*, Vol. 25, (1975), pp. 1071-1076.

Barnes, G. (1979). Vestibulo-ocular function during co-ordinated head and eye movements to acquire visual targets, *Journal Physiol*, Vol. 287, (1979), pp. 127-147.

Becker, W. & Reinhart, J. (1990). Human oblique saccades: Quantitative analysis of the relation between horizontal and vertical components, *Vision Research*, Vol. 30, No. 6, (1990), pp. 893-920.

Bell, A. H.; Meredith, M. A.; Opstal, A. J. V. & Munoz, D. P. (2006). Stimulus intensity modifies saccadic reaction time and visual response latency in the superior colliculus, *Experimental Brain Research*, Vol. 174, No. 1, (2006), pp. 53-59.

Bernstein, N. (1967), *The coordination and regulation of movements*, pp. 196, Oxford, UK, Pergamo, (1967)

Berthouze, L. & Kuniyoshi, Y. (1998). Emergence and Categorization of Coordinated Visual Behavior Through Embodied Interaction, *Autonomous Robots*, Vol. 5, No. 3, (1998), pp. 369-379.

Bizzi, E.; Kalil, R. & Morasso, P. (1972). Two modes of active eye-head coordination in monkeys, *Brain Research*, Vol. 40, (1972), pp. 45-48.

Bizzi, E.; Kalil, R. & Tagliasco, V. (1971). Eye-head coordination in monkeys, No. evidence for centrally patterned organization, *Science*, Vol. 173, (1971), pp. 452-454.

Brooks, R.; Breazeal, C.; Marjanovic, M.; Scassellati, B. & Williamson, M. (1999). The Cog Project: Building a Humanoid Robot, In: *Lecture Notes in Computer Science*, pp. 52-87,

Springer-Verlag.
Bruske, J.; Hansen, M.; Riehn, L. & Sommer, G. (1997). Biologically inspired calibration-free adaptive saccade control of a binocular camera-head, *Biological Cybernetics*, Vol. 77, No. 6, (1997), pp. 433-446.
Collewijn, H.; Erkelens, C. & Steinman, R. (1988). Binocular coordination of human horizontal saccadic eye movements, *The Journal of Physiology*, Vol. 404, No. 1, (1988), pp. 157-182.
Crawford, J. D.; Douglas, Tweed, B. & Vilis, T. (2003). Static ocular counterroll is implemented through the 3-D neural integrator, *Journal of Neurophysiol*, Vol. 90, (2003), pp. 2777-2784.
Freedman, E. & Sparks, D. (2000). Coordination of the eyes and head, No. movement kinematics, *Experimental Brain Research*, Vol. 131, No. 1, (2000), pp. 22-32.
Freedman, E. & Sparks, D. (1997). Eye-head coordination during head-unrestrained gaze shifts in rhesus monkeys, *Journal Neurophysiology*, Vol. 77, (1997), pp. 2328-2348.
Galiana, H. & Guitton, D. (1992). Central organization and modeling of eye-head coordination during orienting gaze shifts., *Annals of the New York Academy of Sciences*, Vol. 656, (1992), pp. 452-471.
Girard, B. & Berthoz, A. (2005). From brainstem to cortex, No. computational models of the saccade generation circuitry, *Progress in Neurobiology*, Vol. 77, No. 4, (2005), pp. 215-255.
Gisbergen, J. V.; Opstal, A. V. & Tax, A. (1985). Experimental test of two models for the generation of oblique saccades, *Experimental Brain Research*, Vol. 57, No. 2, (1985), pp. 321-336.
Gisbergen, J. V.; Opstal, J. V. & Ottes, F. (1984). Parametrization of saccadic velocity profiles in man, *in Theoretical and applied aspects of eye movement research*, Gale, A. G., Johnson, J., (Ed.) Elsevier Science, pp. 87-94, New York
Goossens, H. & Opstal, A. V. (1997). Human eye-head coordination in two dimensions under different sensorimotor conditions, *Experimental Brain Research*, Vol. 114, (1997), pp. 542-560.
Green, D. G. (1970). Regional variations in the visual acuity for interference fringes on the retina. *The Journal of Physiology*, Vol. 207, No. 2, (April 1970) 351–356.
Grossberg, S. & Kuperstein, M. (1986). *Neural dynamics of adaptive sensory motor control: ballistic eye movements*., Elsevier, Amsterdam.
Guitton, D. & Volle, M. (1987). Gaze control in humans, No. eye-head coordination during orienting movements to targets within and beyond the oculomotor range., *Journal of Neurophysiol* , Vol. 58, (1987), pp. 496-508.
Henn, V. (1993). Neural Control of Saccadic Eye Movements, In: *Multisensory control of movement*, Berthoz, A., (Ed.), Oxford University Press, pp. 7-26, Oxford, UK
Kaneko, K.; Kanehiro, F.; Kajita, S.; Hirukawa, H.; Kawasaki, T.; Hirata, M.; Akachi, K. & Isozumi, T. (2004). Humanoid robot HRP-2, *Proceedings of Robotics and Automation*, pp. 1083-1090, ISBN: 0-7803-8232-3 , New Orleans, April 2005.
Kawato, M.; Furukawa, K. & Suzuki, R. (1987). A hierarchical neural-network model for control and learning of voluntary movement, *Biological Cybernetics*, Vol. 57, No. 3, (1987), pp. 169-185.
Laschi, C.; Patane, F.; Maini, E.; Manfredi, L.; Teti, G.; Zollo, L.; Guglielmelli, E. & Dario, P. (2008). An Anthropomorphic Robotic Head for Investigating Gaze Control,

Advanced Robotics, Vol. 22, No. 33, (2008), pp. 57-89.

Laurutis, V. P. & Robinson, D. A. (1986). The vestibulo-ocular reflex during human saccadic eye movements., *The Journal of Physiology*, Vol. 373, (1986), pp. 209-233.

Lefèvre, P.; Bottemanne, I. & Roucoux, A. (1992). Experimental study and modeling of vestibulo-ocular reflex modulation during large shifts of gaze in humans, *Experimental Brain Research*, Vol. 91, No. 3, (1992), pp. 496-508.

Manfredi, L.; Maini, E. S.; Dario, P.; Laschi, C.; Girard, B.; Tabareau, N. & Berthoz, A. (2006). Implementation of a neurophysiological model of saccadic eye movements on an anthropomorphic robotic head, *International Conference on Humanoid Robots, 2006 6th IEEE-RAS*, pp. 438-443, 1-4244-0200-X, Genova, December 2006.

Maini, E. S.; Manfredi, L.; Laschi, C.; Dario, P. (2008). Bioinspired velocity control of fast gaze shifts on a robotic anthropomorphic head, *Autonomous Robots*, Vol. 25, (2008), pp. 37-58.

Ottes, F.; Van Gisbergen J.A. & Eggermont, J. (1986). Visuomotor fields of the superior colliculus, No. a quantitative model, *Vision Research*, Vol. 26, (1986), pp. 857-873.

Pelisson, D.; Prablanc, C. & Urquizar, C. (1988). Vestibuloocular reflex inhibition and gaze saccade control characteristics during eye-head orientation in humans, *Journal of Neurophysiology*, Vol. 59, No. 3, (1988), pp. 997-1013.

Radau, P.; Tweed, D. & Vilis, T. (1994). Three-dimensional eye, head, and chest orientations after large gaze shifts and the underlying neural strategies, *Journal of Neurophysiology*, Vol. 72, (1994), pp. 2840-2852.

Robinson, D. (1972). Eye movements evoked by collicular stimulation in the alert monkey, *Vision Research*, Vol. 12, (1972), pp. 1795-1808.

Robinson, D. A. (1975). Oculomotor control signals, In: *Basic mechanism of ocular motility and their clinical implications,* Lennerstrand, G. D. & and Rita, P. B. (Ed.), pp. 337-374, Pergamon, Oxfork, UK, Pergamon, Oxford

Sparks, D. L. (2002). The brainstem control of saccadic eye movements, *Nature Reviews Neuroscience*, Vol. 3, (2002), pp. 952-964.

Takanishi, A.; Takanobu, H.; Kato, I. & Umetsu, T. (1999). *Development of the Anthropomorphic Head-Eye Robot WE-3RII with an Autonomous Facial Expression Mechanism,*. Proceedings of International Conference on Robotics and Automation, pp. 3255–3260, 0-7803-5180-0, Detroit, October 1999

Tweed, D.; Glenn, B. & Vilis, T. (1995). Eye-head coordination during large gaze shifts, *Journal Neurophysiol*, Vol. 73, (1995), pp. 766-779.

Westheimer, G. & Blair, S. (1973). Oculomotor defects in cerebellectomized monkeys., *Investigative Ophthalmology*, Vol. 12, No. 8, (1973), pp. 618-621.

Wolpert, D. M. & Kawato, M. (1998). Multiple paired forward and inverse models for motor control, *Neural Networks*, Vol. 11, No. 7-8, (1998), pp. 1317-1329.

Zangemeister, W.; Lehman, S. & Stark, L. (1981). Simulation of head movement trajectories: model and fit to main sequence, *Biological Cybernetics*, Vol. 41, No. 1, (1981), pp. 19-32.

Zangemeister, W. H. & Stark, L. (1981). Active head rotations and eye-head coordination, *Annals of the New York Academy of Sciences*, Vol. 374, No. 1, (1981), pp. 540-559.

Zatsiorsky, M. (1998). *Kinematics of Human Motion*, Human Kinetics Europe, United Kingdom.

Zee, D.; Optican, L.; Cook, J.; Robinson, D. & Engel, W. (1976). Slow saccades in spinocerebellar degeneration., *Archives of Neurology*, Vol. 33, No. 4, (1976), pp. 243-251.

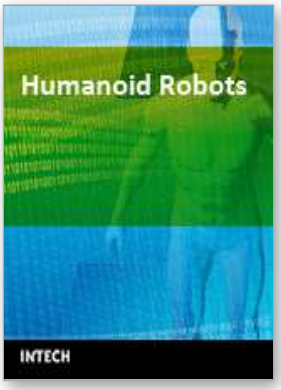

Humanoid Robots
Edited by Ben Choi

ISBN 978-953-7619-44-2
Hard cover, 388 pages
Publisher InTech
Published online 01, January, 2009
Published in print edition January, 2009

Humanoid robots are developed to use the infrastructures designed for humans, to ease the interactions with humans, and to help the integrations into human societies. The developments of humanoid robots proceed from building individual robots to establishing societies of robots working alongside with humans. This book addresses the problems of constructing a humanoid body and mind from generating walk patterns and balance maintenance to encoding and specifying humanoid motions and the control of eye and head movements for focusing attention on moving objects. It provides methods for learning motor skills and for language acquisition and describes how to generate facial movements for expressing various emotions and provides methods for decision making and planning. This book discusses the leading researches and challenges in building humanoid robots in order to prepare for the near future when human societies will be advanced by using humanoid robots.

INTECH
open science | open minds

InTech Europe
University Campus STeP Ri
Slavka Krautzeka 83/A
51000 Rijeka, Croatia
Phone: +385 (51) 770 447
Fax: +385 (51) 686 166
www.intechopen.com

InTech China
Unit 405, Office Block, Hotel Equatorial Shanghai
No.65, Yan An Road (West), Shanghai, 200040, China
中国上海市延安西路65号上海国际贵都大饭店办公楼405单元
Phone: +86-21-62489820
Fax: +86-21-62489821